QM/MM Free Energy Simulations of Salicylic Acid Methyltransferase: Effects of Stabilization of TS-like Structures on Substrate Specificity

Jianzhuang Yao,[†] Qin Xu,[†] Feng Chen,[‡] and Hong Guo*,[†]

Department of Biochemistry and Cellular and Molecular Biology and Department of Plant Sciences, University of Tennessee, Knoxville, Tennessee 37996, United States

Received: September 12, 2010; Revised Manuscript Received: November 23, 2010

Salicylic acid methyltransferases (SAMTs) synthesize methyl salicylate (MeSA) using salicylate as the substrate. MeSA synthesized in plants may function as an airborne signal to activate the expression of defense-related genes and could also be a critical mobile signaling molecule that travels from the site of plant infection to establish systemic immunity in the induction of disease resistance. Here the results of QM/MM free energy simulations for the methyl transfer process in *Clarkia breweri* SAMT (CbSAMT) are reported to determine the origin of the substrate specificity of SAMTs. The free energy barrier for the methyl transfer from *S*-adenosyl-L-methionine (AdoMet) to 4-hydroxybenzoate in CbSAMT is found to be about 5 kcal/mol higher than that from AdoMet to salicylate, consistent with the experimental observations. It is suggested that the relatively high efficiency for the methylation of salicylate compared to 4-hydroxybenzoate is due, at least in part, to the reason that a part of the stabilization of the transition state (TS) configuration is already reflected in the reactant complex, presumably, through the binding. The results seem to indicate that the creation of the substrate complex (e.g., through mutagenesis and substrate modifications) with its structure closely resembling TS might be fruitful for improving the catalytic efficiency for some enzymes. The results show that the computer simulations may provide important insights into the origin of the substrate specificity for the SABATH family and could be used to help experimental efforts in generating engineered enzymes with altered substrate specificity.

Introduction

Plants produce a large number of low molecular weight metabolites, and some of these metabolites play critical roles in diverse biological processes including plant growth and development as well as plant interactions with the environment. Chemical modifications of such metabolites by different enzymes may have a profound impact on these activities. One of such modifications is enzymatic methylation of carboxyl moieties of certain small molecules, such as salicylic acid (SA), benzoic acid (BA), indole-3-acetic acid (IAA), gibberellic acid (GA), farnesoic acid (FA), cinnamic/coumaric acid (CC), and jasmonic acid (JA), using *S*-adenosyl-L-methionine (AdoMet) as the methyl donor.[1] The methylation of carboxyl group of these compounds may affect the concentrations of the free acids in plant tissues, and the corresponding methylated products can have biological and ecological functions that are quite different from their precursors. The enzymes that catalyze the methylation of SA, BA, IAA, GA, FA, CC, and JA, for instance, are SA methyltransferase (SAMT),[2] BA methyltransferase (BAMT),[3] IAA methyltransferase (IAMT),[4] GA methyltransferase (GAMT),[5] FA methyltransferase (SAMT),[6] CC methyltransferase (CCMT),[7] and JA methyltransferase (JAMT),[8] respectively. These enzymes belong to the same SABATH enzyme family[9] (which was named based on the first three identified members of the family, SAMT, BAMT, and theobromine synthase). They can be distinguished according to their substrate preferences and are homologous at the protein sequence level. The SABATH family also contains some other proteins, including the nitrogen-directed methyltransferases involved in caffeine biosynthesis.[10] It has been demonstrated that the emergence of novel SABATH MT activity can occur rapidly and small changes in primary protein sequences can lead to the functional emergence of SABATH proteins with altered substrate preferences.[11] Although the SABATH enzymes have been a subject of extensive biochemical and structural investigations,[2a,11b,12] the factors that determine the substrate specificity and the origin for the differences in the breadth of substrate preference of individual enzymes are still not well understood.

SA methyltransferases (SAMTs) are among the best studied members of the SABATH family that synthesize methyl salicylate (MeSA) using SA as the substrate. The closely related enzymes of the family include BA methyltransferases (BAMTs) which have a higher catalytic efficiency and preference for benzoic acid (BA) lacking the 2-hydroxyl group of SA. It is generally believed that the reactive carboxyl groups of the substrates are fully or predominantly deprotonated at cellular pH values,[11b] and the methyl transfers should occur without enzyme-mediated general acid/base catalysis (Figure 1a). SA is an important plant signal/hormone and can influence a number of processes, including seed germination, seedling establishment, cell growth, respiration, senescence-associated gene expression, responses to abiotic stresses, and fruit yield.[13] Moreover, it has been demonstrated that SA may signal the activation of disease resistance following pathogen infection.[13] MeSA synthesized by SAMT is a volatile ester and is normally absent in plants. However, MeSA can be dramatically induced upon pathogen infection.[14] It has been suggested that MeSA may function as an airborne signal to activate the expression of defense-related

* Corresponding author. E-mail: hguo1@utk.edu.
[†] Department of Biochemistry and Cellular and Molecular Biology.
[‡] Department of Plant Sciences.

10.1021/jp1086812
Published on Web 12/17/2010

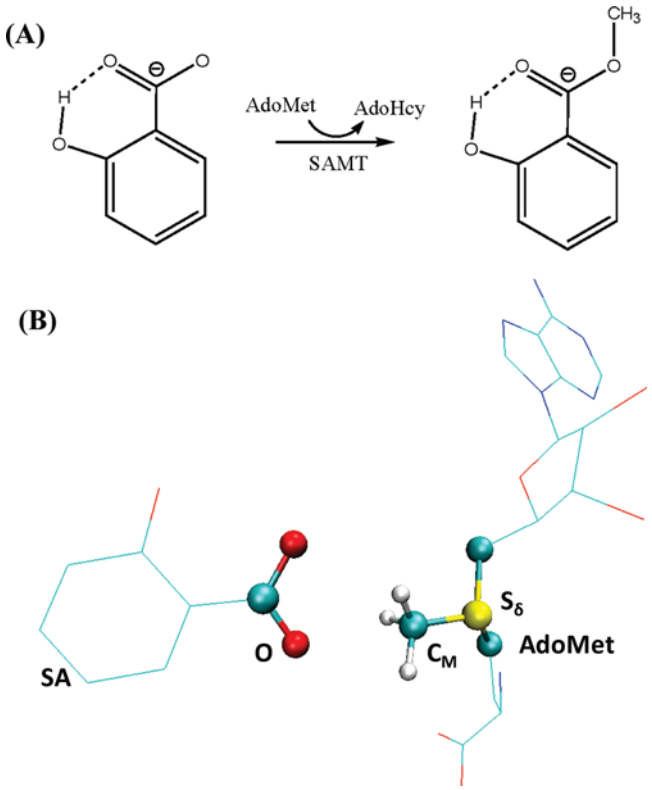

Figure 1. (A) Reaction catalyzed by SAMT. (B) Atoms used for the definition of the reaction coordinate in calculating the free energy profiles of the methyl transfers. The reaction coordinate is $R = r(C_M \cdots S_\delta) - r(C_M \cdots O)$.

genes for disease resistance in nondamaged organs of the same or neighboring plants.[15] Recent studies have also shown that MeSA may be a critical mobile signaling molecule that travels from the site of infection to establish systemic immunity in the induction of a long-lasting and broad-spectrum disease resistance,[16] the so-called systemic acquired resistance (SAR).[17] Furthermore, MeSA is a flavor ingredient for taste and scent of many fruits and flowers and is often produced synthetically and used for making candy, food, and medicine. Given the importance of SA and MeSA in plant biology and food industry, understanding the mechanism of the SA methylation catalyzed by SAMT as well as the origin of its substrate specificity is of considerable interest. Such understanding may also provide important insights into the substrate specificity of other members of the SAMT family whose activities may influence diverse biological processes in plants.

Previous experimental studies[11b,12a] have shown that the substrate recognition and catalytic efficiency of SAMTs and other members of the family appear to have subtle biochemical characteristics, and their dependences on the active site and other residues may be complicated. Therefore, applications of different experimental and computational approaches may be required for quantitatively assessing the structural features for substrate recognition and for identifying the amino acid residues important for the enzyme's function. Computer simulations can provide important insights into the energetic origins of substrate specificity and help to predict the effects of mutations quantitatively, as demonstrated from numerous previous investigations. We have applied molecular dynamics (MD) and free energy (potential of mean force) simulations with hybrid quantum mechanical/molecular mechanical (QM/MM) potentials to study several enzyme-catalyzed reactions earlier, including protein lysine methyltransferases (PKMTs)[18] which belong to another family of AdoMet-dependent methyltransferases and may catalyze the methyl transfer processes from AdoMet to the lysine residues on the tails of histone proteins. It was found that there is a good correlation between the activities of the enzymes observed experimentally and the results of the computer simulations,[18] suggesting the computational approaches are well suited for the investigations of enzyme-catalyzed methyl transfer processes.

Here, we report the results of QM/MM MD and free energy simulations for the methyl transfers in *Clarkia breweri* SAMT (CbSAMT). One of the interesting experimental results is the observation that the catalytic efficiency of SAMTs is considerable lower for 4-hydroxybenzoic acid (4HA) than for SA.[2a,11b,12a,b,d] This experimental result may also be used as an important testing ground in the determination of usefulness of the computational approaches for understanding substrate specificity for the SAMT family. It is still not clear as to why the change of the hydroxyl group from the 2-position (as in SA) to 4-position (as in 4HA) can lead to such large decrease in the activity. For instance, for CbSAMT the activity on 4HA is only 0−0.8% of that on SA.[2a,11b] The free energy simulations reported in this work show that the free energy barrier for the methyl transfer from AdoMet to 4-hydroxybenzoate in CbSAMT is about 5 kcal/mol higher than that from AdoMet to salicylate, consistent with the experimental observations.[2a,11b] The results show that the structure of the reactant complex containing salicylate resembles the transition state (TS) of the reaction with the carboxylate of salicylate well aligned with the methyl group of AdoMet. Thus, a part of the stabilization of the TS configuration is already reflected in the reactant complex, presumably, through the binding. This is, however, not the case for 4-hydroxybenzoate. The existence of the 4-hydroxyl group and the increase of the length of the molecule appear to weaken some of the key hydrogen bonds and produce new repulsions between 4-hydroxybenzoate and some of the neighboring residues (e.g., Phe347). This leads to a poor alignment of the reactive groups in the 4-hydroxybenzoate reactant complex that is considerably different from those of the transition state of the 4-hydroxybenzoate methylation reaction and the reactant complex containing salicylate mentioned above. Thus, additional energy is needed for generating the TS configuration during the methyl transfer, leading to a higher free energy barrier (lower efficiency). To the best of our knowledge, this is the first time that the QM/MM MD and free energy simulations are used for studying the SASBTH family. The results presented here suggest that the computer simulations may provide important insights into the origin of the substrate specificity for this family and could be used to help experimental efforts in generating engineered enzymes with altered substrate specificity in the future.

Methods

QM/MM free energy (potential of mean force) simulations were applied to determine free energy profiles for the methyl transfer from AdoMet to the carboxyl group of salicylate and 4-hydroxybenzoate, respectively, and to characterize the active-site dynamics of the reactant complexes using the CHARMM program.[19] AdoMet/*S*-adenosyl-L-homocysteine (AdoHcy) and the substrates were treated by QM and the rest of the system by MM. The link-atom approach[20] as implemented in CHARMM was applied to separate the QM and MM regions. A modified TIP3P water model[21] was employed for the solvent. The stochastic boundary molecular dynamics method[22] was used for the QM/MM MD and free energy simulations. The system was

separated into a reaction zone and a reservoir region, and the reaction zone was further divided into a reaction region and a buffer region. The reaction region was a sphere with radius r of 20 Å, and the buffer region extended over 20 Å $\leq r \leq$ 22 Å. The reference center for partitioning the system was chosen to be the carboxyl oxygen atom (O) of the substrate where the methyl group is transferred to (see Figure 1a,b). The resulting systems contained around 5600 atoms, including about 400−500 water molecules.

The SCC-DFTB method[23] implemented in CHARMM was used for the QM atoms, and the all-hydrogen CHARMM potential function (PARAM27)[24] was used for the MM atoms. High level ab initio methods (e.g., B3LYP and MP2) are too time-consuming to be used for MD and free energy simulations. To correct the errors due to the deficiency of SCC-DFTB method, an empirical correction approach introduced in the earlier study of PKMT SET7/9[18c] was applied to the free energy curves obtained from the potential of mean force simulations in the present work. This approach has been applied to the studies of PKMT DIM-5[18b] and SET8[18a] previously. In this approach, the results of the SCC-DFTB and B3LYP/6-31G** methods for the description of the methyl transfer in a small model system involving AdoMet and salicylate were compared using an energy minimization-based approach. This comparison allowed us to understand the performance of the semiempirical method in the description of the bond breaking and making for the system under investigation. Some systematic deviations of the SCC-DFTB method in the description of the energetics of the methyl transfer were found from such comparison in the small model system containing AdoMet and salicylate. A simple linear function $\Delta E_{corr} = k_c \times R + E_c$ was derived based on these results and applied to correct the possible errors in the free energy profiles, as was done in the earlier studies of PKMTs.[18] Here, $k_c = 4.4$ kcal mol^{-1} Å^{-1}, $E_c = -5.7$ kcal/mol, and R is the reaction coordinate for the methyl transfer from AdoMet to salicylate (see below). The comparison of the corrected SCC-DFTB and B3LYP/6-31G** potential energy profiles for the methyl transfer in the small model system containing AdoMet and salicylate is given in the Supporting Information. For a more detailed explanation of the correction method and why it may works, see ref 18.

The initial coordinates for the reactant complexes were based on the crystallographic structure (PDB code: 1M6E) of CbSAMT complexed with salicylate and AdoHcy.[11b] A methyl group was manually added to AdoHcy to form AdoMet. In addition, for the reactant complex containing 4-hydroxybenzoate, the hydroxyl group at the 2-position of salicylate was removed and a hydroxyl group was manually added to the 4-position of the ring to generate the substrate. The initial structures for the entire stochastic boundary systems were optimized using the steepest descent (SD) and adopted-basis Newton−Raphson (ABNR) methods. The systems were gradually heated from 50.0 to 298.15 K in 50 ps. A 1 fs time step was used for integration of the equation of motion, and the coordinates were saved every 50 fs for analyses. 1.5 ns QM/MM MD simulations were carried out for each of the reactant complexes. The umbrella sampling method[25] implemented in the CHARMM program along with the weighted histogram analysis method (WHAM)[26] was then applied to determine the changes of the free energy (potential of mean force) as a function of the reaction coordinate for the methyl transfers from AdoMet to the carboxylate groups of salicylate and 4-hydroxybenzoate, respectively. The reaction coordinate was defined as a linear combination of $r(C_M-O)$ and $r(C_M-S_\delta)$ [$R = r(C_M-S_\delta) - r(C_M-O)$] (see Figure 1b for the definitions of the atoms). The determination of multidimensional free energy maps would be too time-consuming. Our previous study[27] indicated that the one-dimensional free energy simulations with the selection of a suitable reaction coordinate reflecting the key bond-breaking making events may be able to capture the key energetic properties for the reaction (e.g., the free energy barrier). For each methyl transfer process, 20 windows were used, and for each window 100 ps simulations were performed with 50 ps equilibration. The force constants of the harmonic biasing potentials used in the PMF simulations were 50−500 kcal mol^{-1} Å^{-2}. The statistical errors for the free energy profiles were also estimated and were found to be quite small (see the Supporting Information).

Results and Discussion

The active-site structures of the reactant complexes for the methyl transfers from AdoMet to salicylate (Figure 2B) and from AdoMet to 4-hydroxybenzoate (Figure 2C) in CbSAMT obtained from the simulations are compared with that of the X-ray structure (Figure 2A). Figure 2B shows that the active-site structure for the salicylate complex generally agrees with the experimental structure shown in Figure 2A. For instance, the position of the reactive carboxylate group of salicylate is fixed by the hydrogen bonds from Trp-151 and Gln-25, and these interactions are expected to be important for an efficient methyl transfer. Comparison of parts A and B of Figure 2 shows that there are some deviations in the positions of the residues and ligand in the two structures. These differences seem to be reasonable due in part to the fact that the experimental structure is not the reactant complex and contains AdoHcy rather than AdoMet. The existence of the methyl group as well as the positive charge on AdoMet is expected to produce some changes in the interactions which could lead to certain modifications in the active site structure. It is interesting to note from Figure 2B that the conserved Lys-10 residue interacts with the carboxylate of salicylate instead of the carbonyl group Met-9 as observed in the X-ray structure.[11b] This seems to suggest that Lys-10 might play a role in the substrate binding, although a detailed investigation is still necessary. The free energy simulations (see below) suggest that Lys-10 is likely to change to the position observed in the X-ray structure and form a hydrogen bond with the carbonyl group of Met-9 during the methyl transfer from AdoMet to salicylate. The result from the simulations is therefore not inconsistent with the X-ray structure. Figure 2B also shows that the methyl group of AdoMet is well aligned with the lone pair of electrons of the carboxylate of salicylate (see also the top figure of Figure 2D), in agreement with the suggestion[11b,28] that SAMT relies on the proper positioning of the SA substrate's ionized and desolvated carboxyl group near the reactive methyl group of SAM to facilitate methyl transfer. Moreover, it has been shown from the previous computational studies[18] on PKMTs that a good alignment between the transferable methyl group and the lone pair of electrons (where the methyl group is transferred to) is an important factor for an efficient methyl transfer for the PKMT enzymes as well. The results of the simulations thus suggest that the requirement for a good alignment of the reactive groups seems to be satisfied for the reactant SAMT complex containing salicylate, consistent with the substrate specificity of this enzyme. As will be discussed below, this reactant structure with the well-aligned reactive groups resembles the transition-state configuration for the methyl transfer so that less free energy would be required for the system to generate such configuration and to reach the transition state.

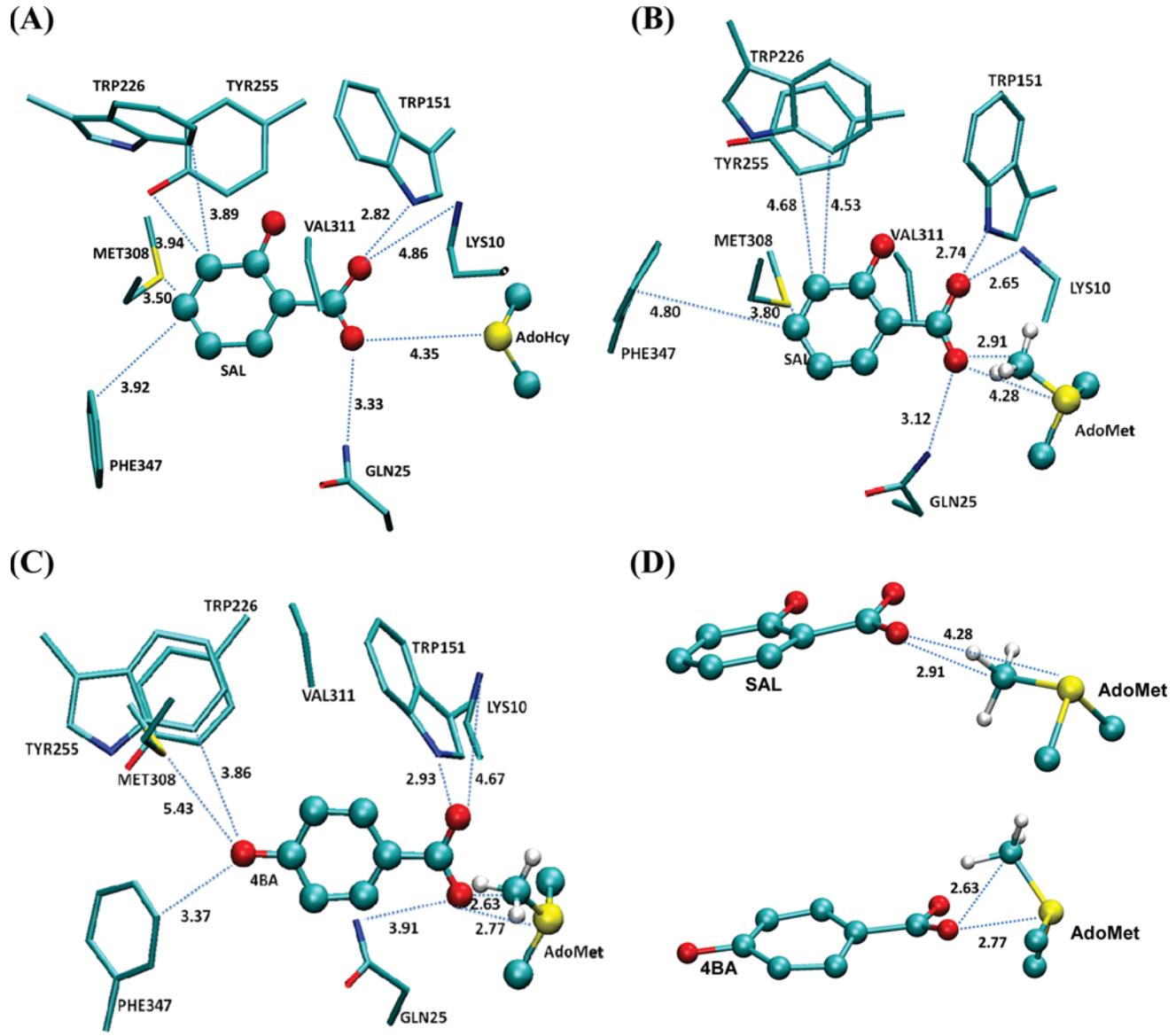

Figure 2. (A) X-ray structure of the active site of CbSAMT complexed with AdoHcy and salicylate. SAMT is shown in sticks, and AdoHcy and salicylate are in balls and sticks. Only the three atoms from AdoHcy and the residues that are close to salicylate are shown for clarity. Some distances are given. (B) Structure of the active site of the reactant complex containing AdoMet and salicylate. Some average distances from the simulations are given. (C) Structure of the active site of the reactant complex containing AdoMet and 4-hydroxybenzoate along with some average distances obtained from the simulations. (D) Relative positions of AdoMet and the substrates in typical structures of the reactant complexes containing salicylate (SAL) (based on Figure 2B) and 4-hydroxybenzoate (4BA) (based on Figure 2C), respectively. Top: salicylate complex. Bottom: 4-hydroxybenzoate complex.

It should be pointed out that a proper balance of different interactions (e.g., the hydrogen bonds involving Trp-151 and Gln-25 and hydrophobic interactions involving Phe-347, Tyr-255, Trp226, and Met-308) is likely to be crucial for producing the good alignment between the reactive groups from the methyl donor and acceptor in the salicylate complex. The change in the substrate structure or replacement of some key residues may destroy such balance and lead to a poor alignment. The structures in Figure 2A,B show that the active site of the enzyme seems to be rather crowded and does not have enough space to accommodate a hydroxyl group at 4-position of the benzoate ring without significant structural modifications. Consistent with this observation, the move of the hydroxyl group from 2- to 4-position in the substrate in going from salicylate to 4-hydroxybenzoate perturbs the active site interactions and changes the active site structure significantly (Figure 2C). For instance, 4-hydroxybenzoate in the reactant complex seems to be pushed toward AdoMet, presumably, by the newly formed interactions of the 4-hydroxyl group with the active site residues (e.g., Phe-347 and Met-308). This movement of the substrate is likely to affect the alignment of the reactive groups. Figure 2D compares the relative orientations of AdoMet and the carboxylate for some typical structures of the reactant complexes containing salicylate (top) and 4-hydroxybenzoate (bottom) obtained from the MD simulations. As is evident from Figure 2D, while a good alignment can be made in the salicylate complex, this is not the case for the 4-hydroxybenzoate complex. The methyl group of AdoMet is pushed away considerably by 4-hydroxybenzoate. The distance between the carboxylate oxygen of 4-hydroxybenzoate and the S_δ atom of AdoMet can reach as small as 2.6 Å. As a result, it is less likely that the methyl group would be able to be located between these two atoms for achieving a good alignment with the lone pair of electrons of the carboxylate and generating the TS-like structure (see below for a more detailed

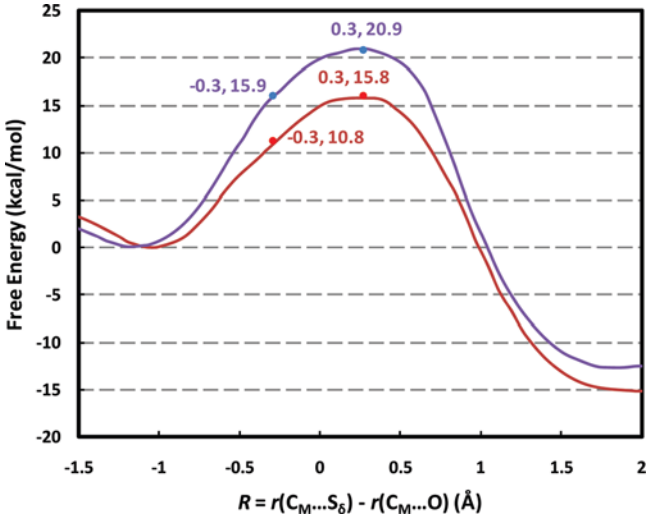

Figure 3. Free energy (potential of mean force) changes for the methyl transfers from AdoMet to salicylate and 4-hydroxybenzoate, respectively, as a function of the reaction coordinate [$R = r(C_M \cdots S_\delta) - r(C_M \cdots O)$] in CbSAMT. The methyl transfer involving salicylate (red). The methyl transfer involving 4-hydroxybenzoate (blue). The relative free energies at $R = -0.3$ and 0.3 Å (near the transition state) are also given.

discussion). The lack of the proper balance of the interactions as a result of the change of the position of the hydroxyl group is presumably the key reason for the deviation of the reactant structure of the 4-hydroxybenzoate complex from the TS-like structure observed for the salicylate complex.

The free energy profiles for the methyl transfers from AdeMot to salicylate and 4-hydroxybenzoate in CbSAMT are plotted in Figure 3 as a function of the reaction coordinate (R). The free energy barriers were calculated to be about 16 and 21 kcal/mol for the salicylate and 4-hydroxybenzoate complexes, respectively. The increase of the free energy barrier from 16 to 21 kcal/mol in going from salicylate to 4-hydroxybenzoate is in good agreement with the experimental finding that the activity of the enzyme on 4HA is only 0−0.8% of that on SA.[2a,11b] The k_{cat} value for the methylation of SA in CbSAMT was estimated to be 0.092 s^{-1}, corresponding to an activation barrier of 18.9 kcal/mol based on the transition-state theory. The calculated free energy barrier (16 kcal/mol) is therefore about 3 kcal/mol lower than this estimated experimental activation barrier. The difference is probably related to the use of density functional approaches in this study that could underestimate the reaction barriers. It should be pointed, however, that the relative free

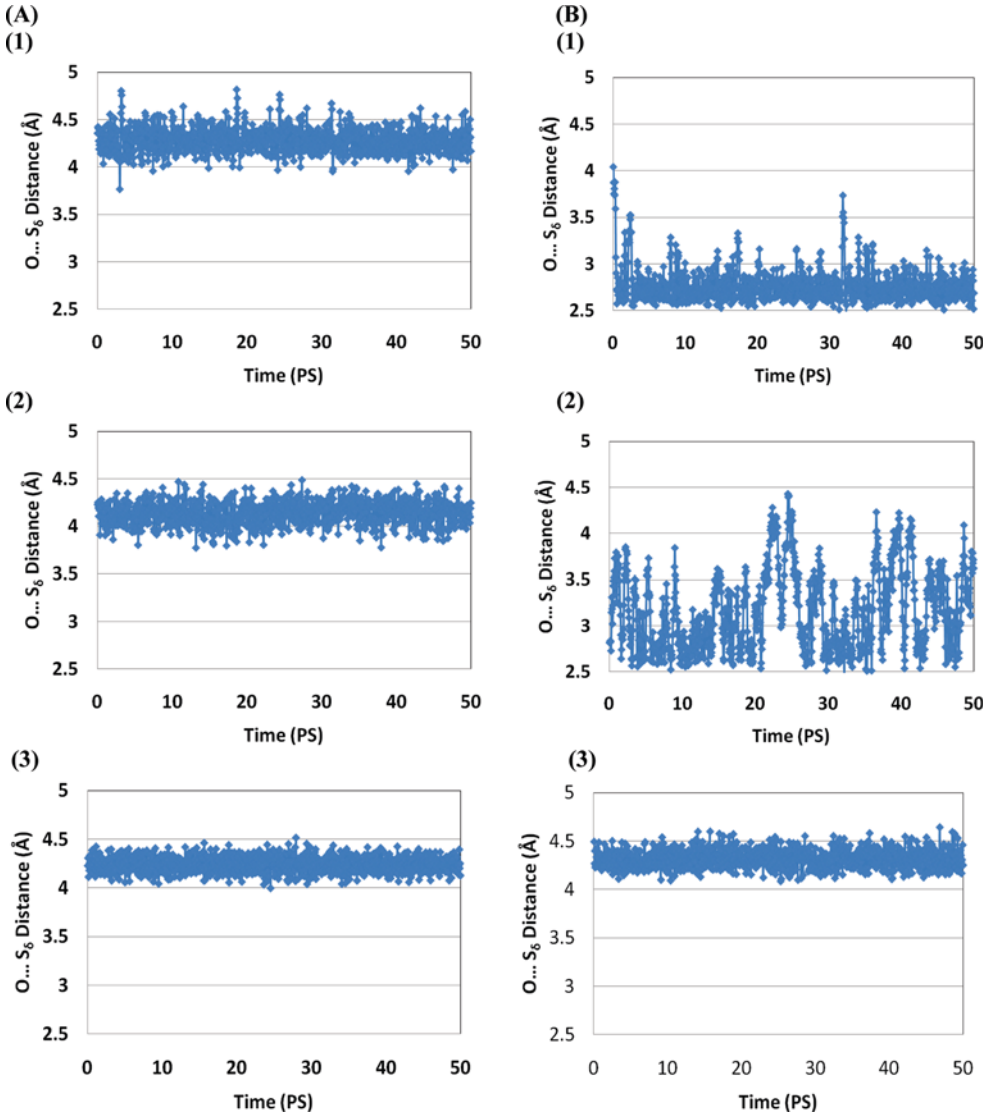

Figure 4. (A) $r(O \cdots S_\delta)$ distance as a function of time for some of the windows during the free energy simulations of the methyl transfer involving salicylate: (1) window 1, (2) window 3, and (3) window 5. (B) $r(O \cdots S_\delta)$ distance as a function of time during the free energy simulations of the methyl transfer involving 4-hydroxybenzoate: (1) window 1, (2) window 3, and (3) window 5.

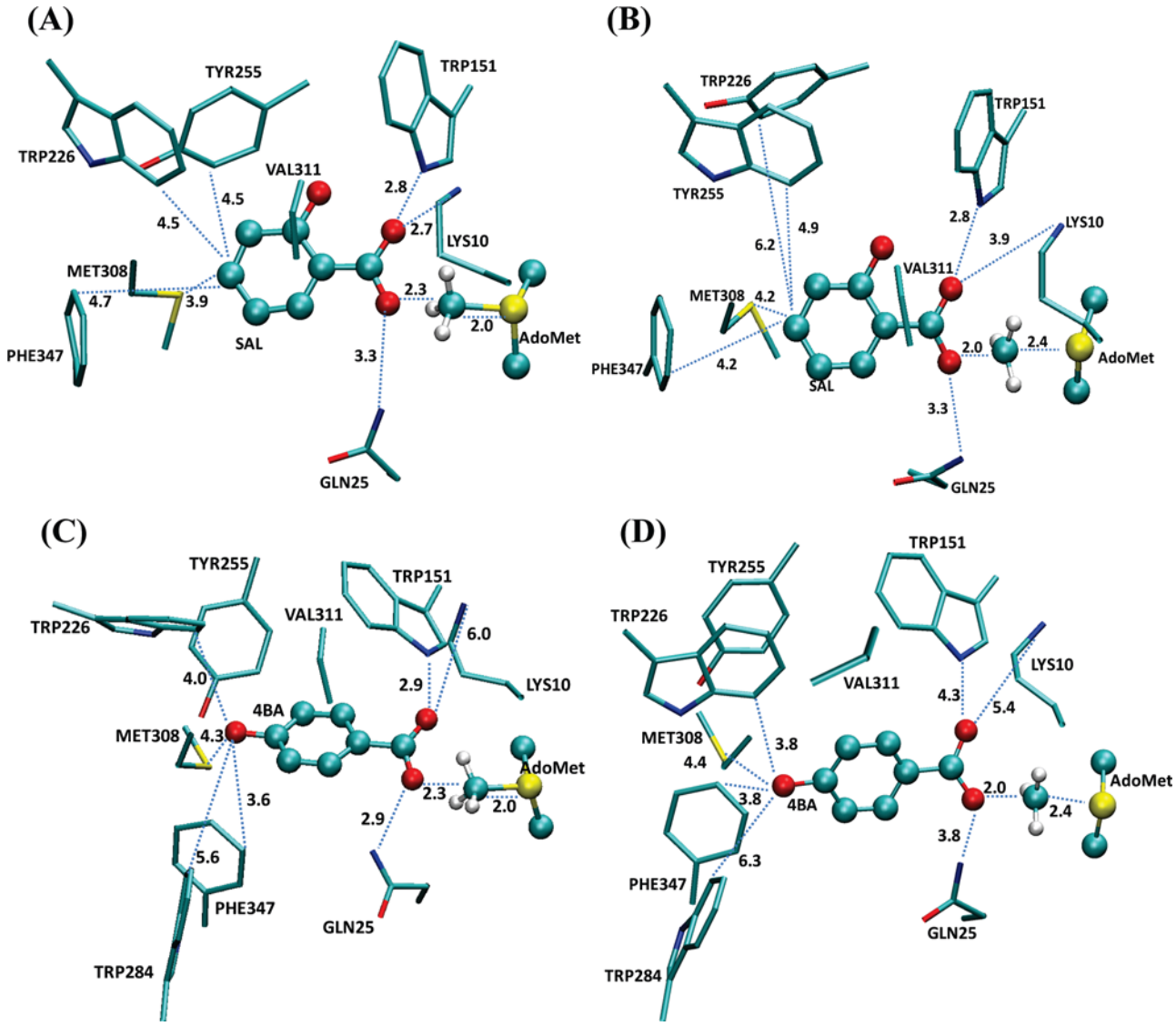

Figure 5. (A) Average structure obtained from window 5 of the free energy simulations for the methyl transfer involving salicylate (see Figure 4A). (B) Average structure near transition state for the methyl transfer involving salicylate. (C) Average structure obtained from window 5 of the free energy simulations for the methyl transfer involving 4-hydroxybenzoate (see Figure 4B). (D) Average structure near transition state for the methyl transfer involving 4-hydroxybenzoate.

energy barriers from the simulations, as opposed to the absolute barriers, are expected to be more important for the comparison of substrate specificities for different molecules. The relative free energy barriers are less sensitive to the choice of the QM method due to the cancellation of the errors and are presumably more reliable. Figure 3 also shows that the increase of the free energy along the free energy profile for the 4-hydroxybenzoate complex occurs well before the system reaches the transition state. Indeed, the free energy difference is already 5 kcal/mol at $R = -0.3$ Å and remains almost the same until the system passes the transition state ($R = 0.3$ Å). The detailed explanation for this result will be given below.

The $r(O\cdots S_\delta)$ distance as a function of time for windows 1, 3, and 5 of the free energy simulations of the methyl transfer involving salicylate and 4-hydroxybenzoate are monitored in parts A and B of Figure 4, respectively. This distance should be at least 4.0−4.5 Å in order to have the transferable methyl group located between O (from the methyl acceptor) and S_δ (from the methyl donor) as required during the methyl transfer. (Note that because the lone pairs of electrons are on the same plane as the carboxylate group, the methyl group should be preferably located on this plane as well.) Figure 4A shows that this condition on $r(O\cdots S_\delta)$ is satisfied for the salicylate complex for the three windows. It can also be shown that this is generally true for almost all the windows (including those near the transition state) during the methyl transfer involving salicylate; the only exceptions are the last few windows near the product state. By contrast, the $r(O\cdots S_\delta)$ distance in the 4-hydroxybenzoate complex remains rather small in general (between 2.5 and 4 Å) in the first two plots (windows 1 and 3), consistent with the structure in Figure 2C. The distance is able to reach relatively large values (e.g., 3.5−4 Å) in some instances in the second plot, suggesting 4-hydroxybenzoate and AdoMet move apart in order to accommodate the methyl group between them as the reaction proceeds. It is of interest to note that the two molecules are able to be 4.0−4.5 Å apart (see the third plot in Figure 4B, corresponding to window 5 in the free energy simulations with $R = -0.3$ Å) well before the system reaches the transition state of the methyl transfer ($\sim R = 0.3$ Å). It should be pointed out that additional energy is expected to be required for achieving this separation of 4-hydroxybenzoate and AdoMet within the enzyme complex during much of the methyl transfer

process. Such energy costs could contribute to the increase of the free energy observed in the free energy profiles in going from salicylate to 4-hydroxybenzoate that covers much of the free energy profile (not just at the transition state), leading to the higher free energy barrier for the methyl transfer involving 4-hydroxybenzoate (see above).

Figure 5 plots the structures at $R = -0.3$ Å and near the transition state ($R \sim 0.3$ Å) for the methyl transfer processes involving salicylate (Figure 5A,B) and 4-hydroxybenzoate (Figure 5C,D), respectively. Comparison of Figure 2C and Figure 5C shows that the local active-site structure seems to have been perturbed during the formation of the TS-like structure, as 4-hydroxybenzoate and AdoMet have to move apart in order to accommodate the methyl group between them (see above). This movement seems to lead to the formation of the hydrogen bond between the carboxylate and Gln25 (Trp151) at $R = -0.3$ Å (see Figure 5C). These hydrogen bonds are broken again near TS (Figure 5D), presumably, due to the neutralization of the negative charge of the carboxylate by the methylene group. It is of interest to note that the relative orientations of the reactive groups (the transferable methyl group and carboxylate) are rather similar for the structures in Figure 5 containing salicylate and 4-hydroxybenzoate; e.g., $r(C_M \cdots O)$ and $r(S_\delta \cdots C_M)$ are 2.0 and 2.4 Å near the transition state, respectively, in the both Figure 5B,D. As discussed earlier, the structural features for the corresponding reactant complexes, on the other hand, are significantly different. Indeed, the relative orientations of the reactive groups in the reactant complex of the salicylate complex (see Figure 2B and the top structure of Figure 2D) are rather close to the corresponding TS-like and TS structures in Figure 5A,B with an average $r(O \cdots S_\delta)$ distance of about 4.3 Å. Thus, a part of the TS stabilization is probably already reflected on the reactant state by generation of such TS-like configuration through the binding. By contrast, the relative orientations of the reactive groups in the reactant complex of the 4-hydroxybenzoate complex (Figure 2C and the bottom structure of Figure 2D) are significantly distorted from those of the corresponding TS-like and TS structures (Figure 5C,D), and the average $r(O \cdots S_\delta)$ distance is only around 2.8 Å. As discussed earlier, the additional energy for generating the TS-like structure for the 4-hydroxybenzoate complex could contribute to the increase of the free energy along the free energy profile (e.g., ~5 kcal/mol at $R = -0.3$ to 0.3 Å) in going from the salicylate to 4-hydroxybenzoate complex, and this leads to the increase of the free energy barrier for the methyl transfer. It would be of interest to replace certain residues and remove some of the interactions that lead to the distorted reactant structure for the 4-hydroxybenzoate complex. The potential residues to be replaced by smaller residues may include Phe-347, Trp284, and Trp226 that are located near the hydroxyl group of 4-hydroxybenzoate (see Figure 5C,D). Additional combined experimental and computational investigations are under way to study the activity of wild-type and mutated enzyme on 4-hydroxybenzoate.

Conclusions

One of the interesting observations from the previous experimental investigations[2a,11b,12a,b,d] is that the catalytic efficiency of SAMTs is considerable lower for 4-hydroxybenzoic acid (4HA) than for salicylic acid (SA). It was not clear as to why the change of the hydroxyl group from the 2-position (as in SA) to 4-position (as in 4HA) could lead to such large decrease in the activity. The free energy simulations reported in this work showed that the free energy barrier for the methyl transfer from AdoMet to 4-hydroxybenzoate in CbSAMT is about 5 kcal/mol higher than that from AdoMet to salicylate, consistent with the experimental observations.[2a,11b] It was found that the structure of the reactant complex containing salicylate is rather close to the corresponding TS structure. Thus, a part of the TS stabilization is probably already reflected in the reactant state by generation of such TS-like configuration through the binding. By contrast, the structure of the reactant complex containing 4-hydroxybenzoate is significantly distorted from the corresponding TS structure. Thus, additional energy seems to be required to generate the TS-like structure during the methyl transfer process. This leads to an upshift of the free energy profile and a higher free energy barrier (lower efficiency) for the methyl transfer. The results seem to indicate that for a given substrate the efficiency of the catalysis might depend on the energy cost for generating the TS-like structure at the active site during the reaction, although other factors may be involved as well. Thus, the creation of the reactant structure (e.g., through mutagenesis and substrate modifications) that requires less energy to generate the TS-like structure in the active site might be fruitful for improving the catalytic efficiency for some enzymes, although stabilization of the charge formation may be important as well (e.g., as observed in the case of cytidine deaminase[29]). The results presented here suggest that the computer simulations may provide important insights into the origin of the substrate specificity for the SABATH family and could be used to help experimental efforts in generating engineered enzymes with altered substrate specificity.

Acknowledgment. We thank Professor Martin Karplus for a gift of the CHARMM program. This work was supported by the National Science Foundation (Grant 0817940 to H.G.), the DOE Office of Biological and Environmental Research - Genome to Life Program through the BioEnergy Science Center (BESC) (to F.C.), and the Sun Grant Initiative (to F.C.). We are also grateful for the computer resources (Newton) from University of Tennessee, Knoxville.

Supporting Information Available: Figures S1 and S2. This material is available free of charge via the Internet at http://pubs.acs.org.

References and Notes

(1) Taiz, L.; Zeiger, E. *Plant Physiology*, 4th ed.; Sinauer Associates: Sunderland, MA, 2006.

(2) (a) Ross, J. R.; Nam, K. H.; D'Auria, J. C.; Pichersky, E. *Arch. Biochem. Biophys.* **1999**, *367*, 9. (b) Chen, F.; D'Auria, J. C.; Tholl, D.; Ross, J. R.; Gershenzon, J.; Noel, J. P.; Pichersky, E. *Plant J.* **2003**, *36*, 577.

(3) Murfitt, L. M.; Kolosova, N.; Mann, C. J.; Dudareva, N. *Arch. Biochem. Biophys.* **2000**, *382*, 145.

(4) (a) Qin, G. J.; Gu, H. Y.; Zhao, Y. D.; Ma, Z. Q.; Shi, G. L.; Yang, Y.; Pichersky, E.; Chen, H. D.; Liu, M. H.; Chen, Z. L.; Qu, L. J. *Plant Cell* **2005**, *17*, 2693. (b) Zhao, N.; Ferrer, J. L.; Ross, J.; Guan, J.; Yang, Y.; Pichersky, E.; Noel, J. P.; Chen, F. *Plant Physiol.* **2008**, *146*, 455. (c) Zhao, N.; Guan, J.; Lin, H.; Chen, F. *Phytochemistry* **2007**, *68*, 1537.

(5) Varbanova, M.; Yamaguchi, S.; Yang, Y.; McKelvey, K.; Hanada, A.; Borochov, R.; Yu, F.; Jikumaru, Y.; Ross, J.; Cortes, D.; Ma, C. J.; Noel, J. P.; Mander, L.; Shulaev, V.; Kamiya, Y.; Rodermel, S.; Weiss, D.; Pichersky, E. *Plant Cell* **2007**, *19*, 32.

(6) Yang, Y.; Yuan, J. S.; Ross, J.; Noel, J. P.; Pichersky, E.; Chen, F. *Arch. Biochem. Biophys.* **2006**, *448*, 123.

(7) Kapteyn, J.; Qualley, A. V.; Xie, Z. Z.; Fridman, E.; Dudareva, N.; Gang, D. R. *Plant Cell* **2007**, *19*, 3212.

(8) Seo, H. S.; Song, J. T.; Cheong, J. J.; Lee, Y. H.; Lee, Y. W.; Hwang, I.; Lee, J. S.; Choi, Y. D. *Proc. Natl. Acad. Sci. U.S.A.* **2001**, *98*, 4788.

(9) D'Auria, J. C.; Chen, F.; Pichersky, E. *Recent Adv. Phytochem.* **2003**, *37*.

(10) (a) Ogawa, M.; Herai, Y.; Koizumi, N.; Kusano, T.; Sano, H. *J. Biol. Chem.* **2001**, *276*, 8213. (b) McCarthy, A. A.; McCarthy, J. G. *Plant Physiol.* **2007**, *144*, 879.

(11) (a) Pichersky, E.; Noel, J. P.; Dudareva, N. *Science* **2006**, *311*, 808. (b) Zubieta, C.; Ross, J. R.; Koscheski, P.; Yang, Y.; Pichersky, E.; Noel, J. P. *Plant Cell* **2003**, *15*, 1704.

(12) (a) Effmert, U.; Saschen brecker, S.; Ross, J.; Negre, F.; Fraser, C. M.; Noel, J. P.; Dudareva, N.; Piechulla, B. *Phytochemistry* **2005**, *66*, 1211. (b) Zhao, N.; Guan, J.; Ferrer, J. L.; Engle, N.; Chern, M.; Ronald, P.; Tschaplinski, T. J.; Chen, F. *Plant Physiol. Biochem.* **2010**, *48*, 279. (c) Tieman, D.; Zeigler, M.; Schmelz, E.; Taylor, M. G.; Rushing, S.; Jones, J. B.; Klee, H. J. *Plant J.* **2010**, *62*, 113. (d) Hippauf, F.; Michalsky, E.; Huang, R. Q.; Preissner, R.; Barkman, T. J.; Piechulla, B. *Plant Mol. Biol.* **2010**, *72*, 311. (e) Pott, M. B.; Hippauf, F.; Saschenbrecker, S.; Chen, F.; Ross, J.; Kiefer, I.; Slusarenko, A.; Noel, J. P.; Pichersky, E.; Effmert, U.; Piechulla, B. *Plant Physiol.* **2004**, *135*, 1946.

(13) (a) Santner, A.; Estelle, M. *Nature* **2009**, *459*, 1071. (b) Vlot, A. C.; Dempsey, D. A.; Klessig, D. F. *Annu. Rev Phytopathol.* **2009**, *47*, 177. (c) Loake, G.; Grant, M. *Curr. Opin. Plant Biol.* **2007**, *10*, 466.

(14) (a) Huang, J.; Cardoza, Y. J.; Schmelz, E. A.; Raina, R.; Engelberth, J.; Tumlinson, J. H. *Planta* **2003**, *217*, 767. (b) Seskar, M.; Shulaev, V.; Raskin, I. *Plant Physiol.* **1998**, *116*, 387.

(15) Shulaev, V.; Silverman, P.; Raskin, I. *Nature* **1997**, *385*, 718.

(16) Park, S. W.; Kaimoyo, E.; Kumar, D.; Mosher, S.; Klessig, D. F. *Science* **2007**, *318*, 113.

(17) Sticher, L.; MauchMani, B.; Metraux, J. P. *Annu. Rev. Phytopathol.* **1997**, *35*, 235.

(18) (a) Chu, Y. Z.; Xu, Q.; Guo, H. *J. Chem. Theory Comput.* **2010**, *6*, 1380. (b) Xu, Q.; Chu, Y. Z.; Guo, H. B.; Smith, J. C.; Guo, H. *Chem.—Eur. J.* **2009**, *15*, 12596. (c) Guo, H. B.; Guo, H. *Proc. Natl. Acad. Sci. U.S.A.* **2007**, *104*, 8797.

(19) Brooks, B. R.; Bruccoleri, R. E.; Olafson, B. D.; States, D. J.; Swaminathan, S.; Karplus, M. *J. Comput. Chem.* **1983**, *4*, 187.

(20) Field, M. J.; Bash, P. A.; Karplus, M. *J. Comput. Chem.* **1990**, *11*, 700.

(21) Jorgensen, W. L.; Chandrasekhar, J.; Madura, J. D.; Impey, R. W.; Klein, M. L. *J. Chem. Phys.* **1983**, *79*, 926.

(22) Brooks, C. L.; Brunger, A.; Karplus, M. *Biopolymers* **1985**, *24*, 843.

(23) (a) Elstner, M.; Porezag, D.; Jungnickel, G.; Elsner, J.; Haugk, M.; Frauenheim, T.; Suhai, S.; Seifert, G. *Phys. Rev. B* **1998**, *58*, 7260. (b) Cui, Q.; Elstner, M.; Kaxiras, E.; Frauenheim, T.; Karplus, M. *J. Phys. Chem. B* **2001**, *105*, 569.

(24) MacKerell, A. D.; Bashford, D.; Bellott, M.; Dunbrack, R. L.; Evanseck, J. D.; Field, M. J.; Fischer, S.; Gao, J.; Guo, H.; Ha, S.; Joseph-McCarthy, D.; Kuchnir, L.; Kuczera, K.; Lau, F. T. K.; Mattos, C.; Michnick, S.; Ngo, T.; Nguyen, D. T.; Prodhom, B.; Reiher, W. E.; Roux, B.; Schlenkrich, M.; Smith, J. C.; Stote, R.; Straub, J.; Watanabe, M.; Wiorkiewicz-Kuczera, J.; Yin, D.; Karplus, M. *J. Phys. Chem. B* **1998**, *102*, 3586.

(25) Torrie, G. M.; Valleau, J. P. *Chem. Phys. Lett.* **1974**, *28*, 578.

(26) Kumar, S.; Bouzida, D.; Swendsen, R. H.; Kollman, P. A.; Rosenberg, J. M. *J. Comput. Chem.* **1992**, *13*, 1011.

(27) Guo, H. B.; Wlodawer, A.; Nakayama, T.; Xu, Q.; Guo, H. *Biochemistry* **2006**, *45*, 9129.

(28) Takusagawa, F.; Fujioka, M.; Spies, A.; Schowen, R. L. In *Comprehensive Biological Catalysis: A Mechanistic Reference*; Sinnott, M., Ed.; Academic Press: London, 1998; Vol. 1.

(29) (a) Guo, H. B.; Rao, N.; Xu, Q.; Guo, H. *J. Am. Chem. Soc.* **2005**, *127*, 3191. (b) Xu, Q.; Guo, H. B.; Gorin, A.; Guo, H. *J. Phys. Chem. B* **2007**, *111*, 6501.

JP1086812